한국기계가공학회지, 제20권, 제1호, pp. 16～24(2021.01) ISSN 1598-6721(Print)
Journal of the Korean Society of Manufacturing Process Engineers, Vol. 20, No. 1, pp. 16~24(2021.01) ISSN 2288-0771(Online)

https://doi.org/10.14775/ksmpe.2021.20.01.016

A Preliminary Study on the Lamination Characteristics of Inconel 718 Superalloy on S45C Structural Steel using LENS Process

Hyun-Sik Kim*, Hyub Lee**, Dong-Gyu Ahn*,#

*Department of Mechanical Engineering, Chosun UNIV.,
**Korea Additive Manufacturing Innovation Center, Korea Institute of Industrial Technology

LENS 공정을 이용한 Inconel 718 초합금의 S45C 구조용강 위 적층 특성 고찰에 관한 기초 연구

김현식*, 이협**, 안동규*,#

*조선대학교 기계공학과, **한국생산기술연구원 3D 제조 혁신 센터

(Received 12 October 2020; received in revised form 10 November 2020; accepted 16 November 2020)

ABSTRACT

A laser-engineered net shaping (LENS) process is a representative directed energy deposition process. Deposition characteristics of the LENS process are greatly dependent on the process parameters. The present paper preliminarily investigates deposition characteristics of Inconel 718 superalloy on S45C structural steel using a LENS process. The influence of process parameters, including the laser power and powder feed rate, on the characteristics of the bead formation and the dilution in the vicinity of the deposited region is examined through repeated experiments. A processing map and feasible deposition conditions are estimated from viewpoints of the aspect ratio, defect formation, and the dilution rate of the deposited bead. Finally, an appropriate deposition condition considering side angle, deposition ratio, and buy-to-fly (BTF) is predicted.

Keywords : Laser Engineered Net Shaping Process(LENS 공정), Inconel 718 Superally Powder(IN718 초합금 분말), S45C Structural Steel(S45C 구조용강), Deposition Characteristics(적층 특성), Process Parameter (공정 변수)

1. Introduction

The Laser Engineered Net Shaping (LENS) process is the first Directed Energy Deposition (DED) process developed by the Sandia National Laboratories in the United States. The LENS process has been commercialized by Optomec[1,2].

In the LENS process, the laser is irradiated on the substrate or the previously created layer using a coaxial nozzle, in which the focus of the powder injection is the same as the focus of the laser beam, as a heat source and the powder supply nozzle, and, simultaneously, the powder is sprayed

Corresponding Author : smart@chosun.ac.kr
Tel: +82-62-230-7043, Fax: +82-62-230-7243

on the molten pool formed in the substrate or the previously created layer to generate a rapidly heated mixing layer. Subsequently, the deposited region is formed through a rapid cooling of the mixing layer[3,4]. The typical cooling rate in the DED process, including the LENS process, ranges from 103 °C/s to 105 °C/s[5]. Major applications of the LENS process include three-dimensional manufacturing of metal products, repair, restoration, remanufacturing, and hardfacing[1-3,6,7].

Suitable deposition conditions of the LENS process is significantly dependent on the combination of used powders and substrates[8.9]. In addition, various process parameters of the LENS process, including the power of laser, beam diameter of laser, laser travel speed, feed rate of powders, track overlap ratio, and deposition path, deposition characteristics[9-16]. Kummailil et al. investigated the effects by laser power, powder feed rate, laser scan speed, and hatch spacing on the layer thickness in the LENS process[12]. Ferguson et al. deposited SUS 420 stainless steel powder on AISI 1045 steel using the LENS process, in order to investigate the effects of the travel speed of the laser beam and the feed rate of the powders on the width, the depth, and the porosity of the deposited region[13]. Paul et al. experimentally analyzed the effects of the interaction time and the feed rate of powders on the deposition rate and powder catchment efficiency for the deposition of Colmonoy-6 hardfacing alloy using the LENS process[14]. Xiong et al. investigated the effects of the focal distance of the laser beam on the width and the thickness of the deposited bead[15]. Lu et al. examined changes in the shape of the deposited bead, the deposition height according to the power and the travel speed of the laser beam, and the feed rate of powders when the AISI 316L stainless steel is deposited using the LENS process[16]. From results of the investigtion of previous research works, it was revealed that the power of the laser, the travel speed of the laser and the feed rate of powders are major process parameters of the LENS process[9-16]. In addition, it was noted that the ratio of the travel speed and the feed rate greatly affect the deposition rate[14,16].

This study experimentally investigates deposition characteristics of Inconel 718 superalloy on S45C structural steel using a LENS process. The influence of process parameters, including the laser power and powder feed rate, on the characteristics of the bead formation and the dilution in the vicinity of the deposited region is examined. A processing map and feasible deposition conditions are estimated from viewpoints of the aspect ratio, defect formation, and the dilution rate of the deposited bead. Finally, an appropriate deposition condition considering side angle, deposition ratio, and buy-to-fly (BTF) is predicted.

2. Deposition Experiments

In deposition experiments, Inconel 718 (IN718) powders and S45C structural steel are used as the deposition material and the substrate, respectively. Tables 1 and 2 show chemical components of IN718 powders and S45C structural steel, respectively. IN718 powders manufactured by AMC in China is used[17]. The diameter of IN718 powders ranges from 50 μm to 150 μm[17]. A 5-axis hybrid additive manufacturing (AM) system, including a LENS modular print engine (Optomac), of 3D

Table 1 Chemical compositions of IN718 (wt%)[17]

Fe	Ni	Cr	Nb	Mo	Ti	Al	Co	Cu
Balance	53.19	18.34	5.06	3.05	1.05	0.53	0.16	0.08

Table 2 Chemical compositions of S45C (wt%)[18]

Fe	C	Si	Mn	P	S	Cr
Balance	0.42-0.48	0.15-0.35	0.60-0.90	≤0.03	≤0.035	≤0.20

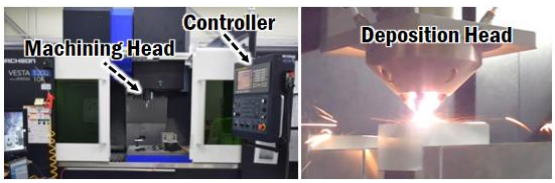

Fig. 1 Hybrid AM system for experiments

Printing Manufacturing Innovation Center (Siheung) of Korea Institute of Industrial Technology (KITECH) is used. In this AM system, the LENS modular printer engine performs deposits metallic materials through 3-axis movement. In addition, the hybrid AM system performs 5-axis cutting of the material through 3-axis linear feed of the cutting head and the rotation of 2-axis rotary table.

Table 3 shows deposition conditions for experiment. The travel speed (V) and diameter (φ) of the laser beam are set to be 1,000 mm/min and 1.0 mm, respectively. Argon (Ar) gas is used as a shield gas to prevent the oxidation of the deposited region and the invasion of the impurity. Dass et al. reported that three major process parameters of the powder feeding type DED process were the power of the laser beam (P), the travel speed of the laser beam (V), and the feed rate of powders (F)[2]. In addition, they also reported that the ratio of the travel speed and the feed rate greatly affected the formation of the deposited region and the occurrence of pores. This study selects the power of the laser beam and the feed rate of the powders as the deposition parameter. The travel speed of laser beam is fixed at 1,000 mm/min. The power of the laser beam and the feed rate of the powders range from 250–500 W and 5.8–12.6 g/min, respectively.

Single deposition beads are created on a S45C substrate according to the combination of the power

Table 3 Deposition conditions for experiments

P(W)	V(mm/min)	F(g/min)	φ (mm)	Shield gas
250-500	1,000	5.8-12.6	1.0	Ar

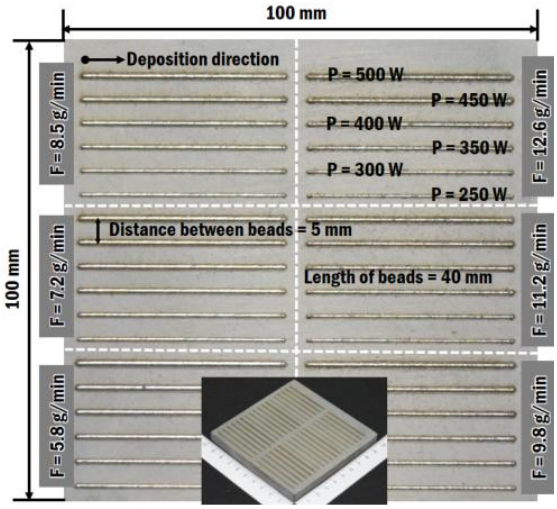

Fig. 2 Specimen design and experimental method

and the feed rate, as shown in Fig. 2. Dimensions of the substrate is 100 mm × 100 mm × 10 mm. The length of the deposited bead and the spacing between beads are set to be 40 mm and 5 mm, respectively. A sandblasting process is applied to the specimen as a pre-treatment for the deposition experiment.

The deposition experiment varies the power of the laser beam from a high power to a low power for each the feed rate of powders (F) when the deposited region changes from top to bottom regions, as shown in Fig. 2. Through the deposition experiments, the bead shape, the mixing ratio (ϖ), side angle of the bead (θ), deposition rate (δ), and BTF (λ) are estimated. The BTF is the ratio of the weight of the purchased raw material and that of the finally manufactured product, which is one of the major measures for the material consumption rate and the deposition rate of the metal AM process. Three specimens are prepared for each deposition condition.

The width, the depth and the inclination angle of the bead are selected as characteristic measures of the bead formation. The values of the characteristics measures for the bead formation and the depth of

the diluted region are measured using an optical microscope. The aspect ratio of the bead (Ω) is defined as the ratio of the width of the bead (W) and the height of the bead (H), as shown in Equation (1). The mixing ratio is predicted by the ratio of the height of the bead and the depth of the dilution (D), as shown in Equation (2)[2]. The BTF of the deposited bead is estimated from the ratio of the feed rate of the powders and the deposition rate, as shown in Equation (3). The deposition rate per is calculated using the density (ρ) of IN718, the travel speed of the laser beam, the width of the deposited bead, and height of the deposited bead, as shown in Equation (4). In order to estimate a cross-sectional area of the deposited beads, the cross section of the deposited beads is assumed as the half area of the ellipse.

$$\Omega(\%) = \frac{H}{W} \tag{1}$$

$$\varpi(\%) = \frac{D}{(H+D)} \times 100 \tag{2}$$

$$\lambda(\%) = \frac{F}{\delta} \times 100 = \frac{F}{\rho A V} \times 100 \tag{3}$$

$$\delta = \frac{\pi \rho V W H}{4} \tag{4}$$

3. Results and Discussion

3.1 Bead Shape

Fig. 3 shows cross-sectional shapes of the deposited beads and the diluted regions for different combinations of the power of the laser beam and the feed rate of powders. Fig. 4(a) and 4(b) show the effects of the power of the laser beam and the feed rate of the powders on the height and width of the deposited bead. The height of the deposited bead also increases when the power of the laser beam and the feed rate of the powders increase. However, the width of the deposited bead increases when the power of the laser beam augments, while the change in the width of the deposited bead was negligible when the feed rate of the powders increases. In addition, the depth of the diluted region increases when the power of the laser beam augments. These phenomena are attributed the fact

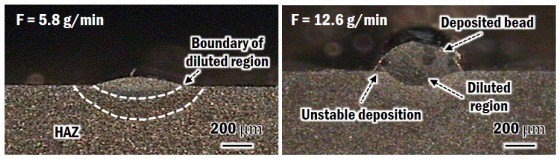

(a) P = 250 W

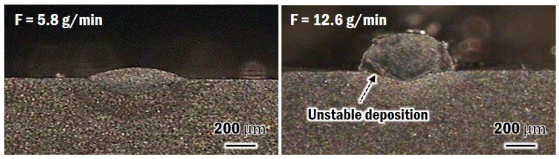

(b) P = 300 W

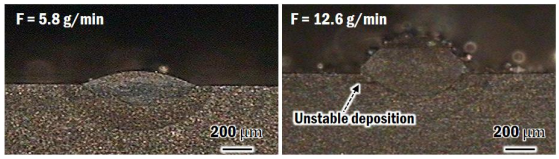

(c) P = 350 W

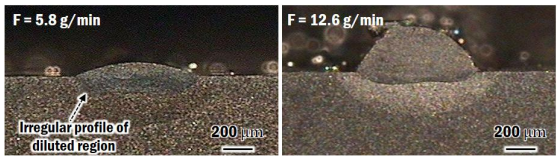

(d) P = 400 W

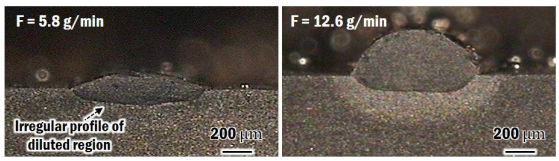

(e) P = 450 W

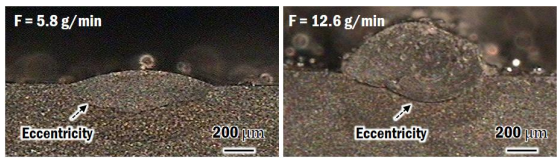

(f) P = 500 W

Fig. 3 Formations of bead and diluted region for different powers of laser and feed rate of powders

that the volume of the molten pool in the substrate increases resulting in a simultaneous increase in the width of the deposited bead and the amount of mixing ratio of materials of the substrate and the powdes in the molten pool when the power of the laser beam augments. In addition, these phenomena are ascribed the fact that the height of the bead increases through the increase in the deposited volume of the powders created on the substrate when the feed rate of powders augments, while the volume of the molten pool is nearly identical when the feed rate of powders augments. From these results, it is noted that the power of the laser beam affects the width of the deposited bead, the height of the deposited bead, the depth of the diluted region. In addition, it is revealed that the feed rate of the powders affects the height of the deposited bead.

An unstable deposition, including partial penetration as well as inappropriate joining between the deposited bead and the substrate, appears when the feed rate of powders is greater than 9.8 g/min and the power of the laser beam is less than 350 W, as shown in Fig. 3(a), 3(b) ad 3(c). For the case of the power of the laser powder of 400 W, unstable deposition occurs when the feed rate is less than 7.2 g/min, as shown in Fig. 3(d). For the case of the power of the laser powder of 450 W, the eccentricity of the diluted region when feed rates of powders are 9.8 g/min and 11.2 g/min, as shown in Fig. 3(e). This is ascribed that unevenness occurs in the vicinity of boundary between the diluted region and the substrate when the feed rate of powders is less than 11.2 g/min. In addition, unevenness at the boundary and eccentricity of the diluted region observed in all feed rates for experiments when the power of the laser is 500 W, as shown in Fig. 3(f).

Fig. 4(c) shows the effects of the power of the laser beam and the feed rate of powders on the aspect ratio of the deposited bead. The aspect ratio is almost identical when the feed rate of powders is

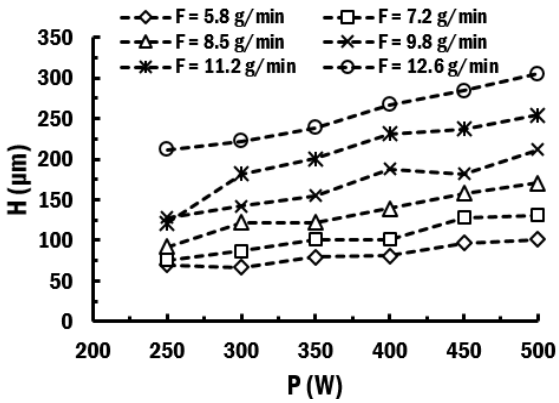

(a) Height of bead

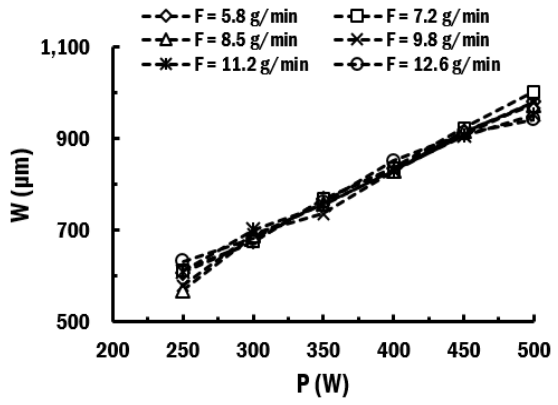

(b) Width of bead

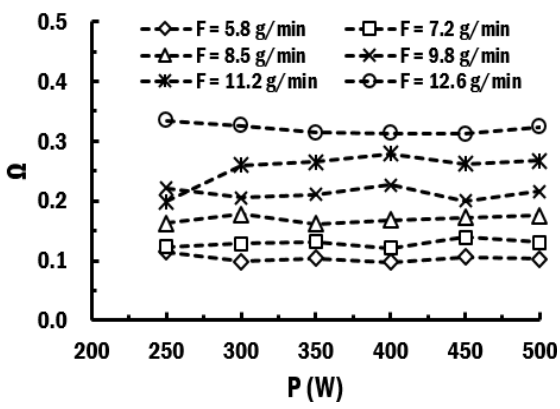

(c) Aspect ratio

Fig. 4 Effects of the power of laser and the feed rate of powders on the height, the width and the aspect ratio of the deposited

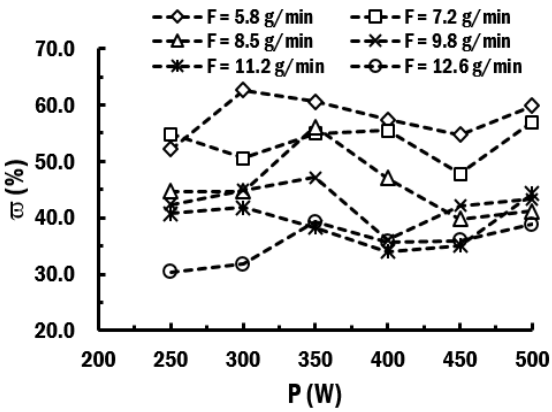

Fig. 5 Effects of the power of laser and the feed rate of powders on the dilution ratio

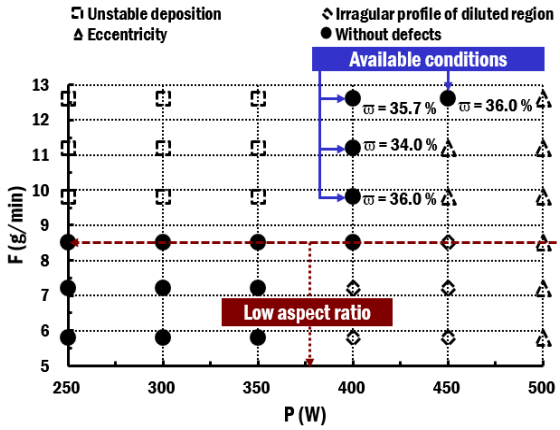

Fig. 6 Processing map for Inconel 718 deposition on S45C substrate using a LENS process

constant. The aspect ratio of the deposited bead by the LENS process is typically greater than 0.15. Considering the typical aspect ratio of the deposited bead, it is revealed that the feed rate should be greater than 8.5 g/min in the power range of the laser beam of the deposition experiments.

3.2 Dilution Ratio

Dilution ratios of the deposited region for different combinations of the power of the laser beam and the feed rate of the powders are estimated, as shown in Fig. 5. A dilution of 10 % an over is required to prevent pores generating due to lake of fusion of the fed material and the substrate in a DED process[2]. The dilution ratio of the deposited region is greater than 30 % for all combinations of the power and the powder feed of this study, as shown in Fig. 5. From these results, it is revealed that the probability of occurrence of pores due to insufficient melting of the substrate is significantly low for deposition conditions for the experiments.

3.3 Processing Map

Using the results of the investigation of the bead formation and the dilution ratio, a processing map based on the powder of the laser beam and the feed rate of powders is predicted for the deposition of IN718 powders on the S45C substrate using the LENS process, as shown in Fig. 6. A combination of the power and the feed rate, which satisfies two mandatory conditions, is chosen as an available deposition condition. The first mandatory condition for the available deposition condition is that deposition defects hardly appear. The second mandatory condition is that the aspect ratio of the deposited bead is greater than a critical value. Although the deposition defects hardly occur, the aspect ratio of the deposited bead is less than 0.15 when the power of the laser beam and the feed rate of powders are less than 350 W and 8.5 g/min, respectively. In addition, despite the deposition defects hardly appear, the aspect ratio of the deposited bead is under 0.15 when the power of the laser beam and the feed rate of powders are 400 W and 8.5 g/min, respectively. Hence, these conditions are excluded from available deposition conditions.

Fig. 6 shows estimated available deposition conditions. The available power of the laser beam is estimated to be 400 W when the feed rate of powders lies in the range of 9.8–12.6 g/min. The available power of the laser beam is predicted to be

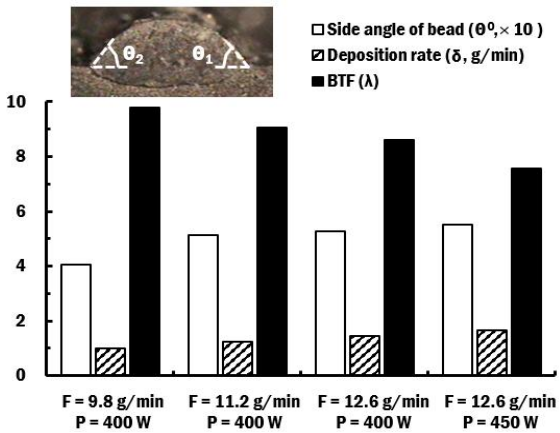

Fig. 7 Side angles, deposition rates and BTFs for different feasible deposition conditions

450 W when the powder feed rate is 12.6 g/min. The dilution ratio lies in the range of 34–36% in estimated available deposition conditions.

3.4 Side Angle, Deposition Rate, BTF, and Appropriate Deposition Conditions

The side angle, the deposition rate and the BTF of the deposited bead for estimated available depositions are compared, as shown in Fig. 7. The side angle of the bead is estimated using Equation (5). Angles of the left side (θ_1) and the right side (θ_2) are indicated in Fig. 7. In estimated available deposition conditions, the side angle, the deposition rate, and BTF lie in ranges of 40.6–55.1 °, 1.0–1.7 g/min, and 7.6–9.8, respectively. The side angle and the deposition rate of the bead increase when the feed rate of powders augments with the BTFs decrease when the feed rate of powders increases, as shown in Fig. 7.

$$\theta = \frac{\theta_1 + \theta_2}{2} \quad (5)$$

In order to improve joining characteristics between the deposited bead and the substrate, and the deposition rate of the fed IN718 powders, the side angle and the deposition rate of the bead should be maximized while the BTF should be minimized. Using these two viewpoints, the combination of the laser power of 450 W and the powder feed rate of 12.6 g/min is chosen as an appropriate deposition conditions. From the results of deposition experiments, characteristic data, including the width of the bead, the height of the bead, the dilution ratio of the diluted region, the width of heat affected zone (W_{HAZ}), the depth of heat affected zone (D_{HAZ}), and the side angle of the bead, the deposition rate of the bead, and BTF can be obtained for the estimated appropriate deposition conditions, as shown in Table 4.

Table 4 Characteristic data for an appropriate deposition condition (P = 450 W and F = 12.6 g/min)

W (μm)	H (μm)	D (μm)	W_{HAZ} (μm)	D_{HAZ} (μm)	Θ (°)	δ (g/min)	BTF
912	284	160	1,220	364	55.1	1.7	5.5

4. Conclusions

This study experimentally investigates the influence of the power of the laser beam dn the feed rate of powders on deposition characteristics of Inconel 718 superalloy on S45C structural steel using a LENS process. From the results of the experiments, following conclusions were obtained:

1. The height and the width of the deposited bead, and the depth of the diluted region increased when the laser power augmented. However, the height of the deposited bead increased when the powder feed rate augmented, whereas the width of the deposited bead and the depth of the diluted region were nearly identical when the powder feed rate augmented.

2. Through the investigation of the defect occurrence of the diluted region and the variation of the aspect ratio of the deposited region according to the power of the laser beam and the feed rate of powders, a combination of the power and the feed rate without defects could be predicted. From this result, it was revealed that the feed rate should be greater than 9.8 g/min to create the desired deposition bead with an aspect ratio greater than a critical value.
3. Through the examination of the dilution ratio of the deposited region, it was revealed that the probability of occurrence of pores due to insufficient melting of the substrate is significantly low for deposition conditions for the experiments.
4. The processing map was estimated from the results of investigation of the occurrence of defects in the deposited region. In addition, available deposition conditions could be predicted.
5. Comparing the side angle of the bead, the deposition rate of the bead, and the BTF of the bead for the estimated available deposition conditions, the combination of the laser power of 450 W and the powder feed rate of 12.6 g/min was selected as an appropriate deposition condition.

In future, the influence of deposition parameters on the morphology, the hardness, and the residual stress distribution of the deposited region will investigate through additional experiments and analysis. Through this investigation, the optimal deposition conditions considering morphology and residual stress distributions will be predicted.

Acknowledgements

"This study was supported by research fund from Chosun University (2020)."

References

1. Ahn, D. G., "Direct Metal Additive Manufacturing Processes and Their sustainable Applications for Green Technology: A Review," International Journal of Precision Engineering and Manufacturing-Green Technology, Vol. 3, No. 4, pp. 381-395, 2016.
2. Dass, A. and Moridi, A., "State of the Art in Directed Energy Deposition: From Additive Manufacturing to Materials Design," Coatings, Vol. 9, No. 7, pp. 418, 2019.
3. Sames, W. J., List, F. A., Pannala, S., Dehoff, R. R. and Babu, S. S., "The Metallurgy and Processing Science of Metal Additive Manufacturing," International Materials Review, Vol. 61, No. 5, pp. 315-360, 2016.
4. Onuike, B., Heer, B., and Bandyopadhyay, A., "Additive Manufacturing of Inconel 718—Copper Alloy Bimetallic Structure Using Laser Engineered Net Shaping (LENS™)," Additive Manufacturing, Vol. 21, pp. 133–140, 2018.
5. Gibson, I., Rosen, D. and Strucker, B., Directed Energy Deposition Process, Additive Manufacturing Technology, Springer, pp. 245-268, 2015
6. Onuike, B., and Bandyopadhyay, A., "Additive Manufacturing in Repair: Influence of Processing Parameters on Properties of Inconel 718," Material Letters, Vol. 252, pp. 256–259, 2019.
7. Wilson, J. M., Piya, C., Shin, Y. C., Zhao, F., and Ramani, K., "Remanufacturing of Turbine Blades by Laser Direct Deposition with Its Energy and Environmental Impact Analysis," Journal of Cleaner Production, Vol. 80, pp. 170–178, 2014.
8. Krishna, B. V. and Bandyopadhyay, A., "Surface Modification of AISI 410 Stainless Steel Using Laser Engineered Net Shaping (LENS™)," Materials & Design, Vol. 30, No. 5, pp. 1490-1496, 2009.

9. Wołosz, P., Baran, A., and Polański, M., “The Influence of Laser Engineered Net Shaping (LENS™) Technological Parameters on the Laser Deposition Efficiency and Properties of H13 (AISI) Steel,” Journal of Alloys and Compounds, Vol. 823, 153840, 2020.
10. Jinoop, A. Paul, C. and Bindra, K. S., “Laser-assisted Directed Energy Deposition of Nickel Super Alloys; A Review,” Proceedings of the Institution of Mechanical Engineers, Part L: Journal of Materials: Design and Applications, Vol. 223, No. 11, pp. 2376-2400, 2019.
11. Izadi, M., Farzaneh, A., Mohammed, M., Gibson, I., and Rolfe, B., “A Review of Laser Engineered Net Shaping (LENS) Build and Process Parameters of Metallic Parts,” Rapid Prototyping Journal, Vol. 26, No. 6, pp. 1059-1078, 2020.
12. Kummailil, J., Sammarco, C., Skinner, D., Brown, C. A., and Rong, K., “Effect of Select LENS™ Processing Parameters on the Deposition of Ti-6Al-4V,” Journal of Manufacturing Processes, Vol. 7, No. 1, pp. 42-50, 2005.
13. Ferguson, J. B., Schultz, B. F., Moghadam, A. D., and Rohatgi, P. K., “Semi-empirical Model of Deposit Size and Porosity in 420 Stainless Steel and 4140 Steel Using Laser Engineered Net Shaping,” Journal of Manufacturing Processes, Vol. 19, pp. 163-170, 2015.
14. Paul, C. P., Jain, A., Ganesh, P., Negi, J., and Nath, A. K., “Laser Rapid Manufacturing of Colmonoy-6 Components,” Optics and Lasers in Engineering, Vol. 44, No. 10, pp. 1096–1109, 2006.
15. Xiong, Y., Smugeresky, J. E. and Schoenung, J. M., “The Influence of Working Distance on Laser Deposited WC-Co,” Journal of Materials Processing Technology, Vol. 209, No. 10, pp. 4935-4941, 2009.
16. Lu, Z. L., Li, D. C., Lu, B. H., Zhang, A. F., Zhu, G. X., and Pi, G., “The Prediction of the Building Precision in the Laser Engineered Net Shaping Process Using Advanced Networks,” Optics and Lasers in Engineering, Vol. 48, No. 5, pp. 519–525, 2010.
17. http://www.amc-powder.com/2017/Nickel_Alloy_Powders_0601/6.html
18. KS D 3752: Carbon Steels for Machine Structural User, SM45C Chemical Composition, Standards and Properties, http://steeljis.com/korea/ks_steel_datasheet.php?name_id=232